A PRELIMINARY STUDY OF THERMO-MECHANICAL STABILITY OF CARBON S-PHASE FORMED IN AUSTENITIC STAINLESS STEEL[1]

Wei Li[2]
Yu Long Chiu[3]
Hanshan Dong[3]

Abstract

Carbon S-phase was generated in the surface of AISI316 austenitic stainless steel by plasma carburising at 500°C for 10h in a gas mixture of 1.5%CH_4 and 98.5%H_2. The thermo-mechanical stability of the carbon S-phase was studied by stressing the 'dog-bone' tensile specimens in the range of 0-200MPa at temperatures ranging from 400 to 500°C for 100-150h. Post-test characterisation was conducted using XRD, SEM, TEM and micro-indentation. The experimental results demonstrate that when tested at a fix temperature the thickness of the carbon S-phase layer increased with the stress applied to the tensile specimens during the thermo-mechanical stability tests. This indicates that tensile stress promotes the diffusion of carbon in the carbon-S-phase. When stressed at 400°C the microstructure of the carbon S-phase was not affected by the stress level; however, when stressed at 450 and 500°C for 100MPa or above, the corrosion resistance of the carbon S-phase slightly deteriorated. The application of a tensile stress during annealing of S-phase layer can retard the deduction of its hardness. This is believed to be related to the early stage precipitation of carbides in the S-phase, which could be facilitated by the applied tensile stress during thermal annealing.

Keywords: Plasma carburising; S-phase; Stability; Stress.

1 INTRODUCTION

Due to the good ductility, weldability and excellent resistance to corrosion, austenitic stainless steel (ASS) are widely used in many industrial sectors, such as nuclear power stations or biomedical devices. However, the relative low hardness of these materials renders the restriction of their broader applications in specific conditions which require outstanding wear resistance and load bearing capacity. Therefore, the enhancement of the surface properties of ASS has been an intensive research subject. It has been proved that nitriding or carburizing of ASSs at relative low temperature (below about 500°C for carburizing and even lower for nitriding) could form a layer bearing good mechanical and tribological properties and anti-corrosion ability as well.[1,2] This precipitation-free layer super-saturated by interstitial atoms(about 12at% carbon or 25at% nitrogen) was called the S phase[3,4] and expanded or supersaturated austenite.[5,6]

Although S-phase exhibits excellent property and has expanded the application of ASS,[7] it is metastable and will change to more stable phase under certain conditions. For example, Li and Dong[8] have reported that precipitation of chromium carbides or nitrides occurred when S-phase was annealed above a certain level of temperatures. Consequently, S-phase was decomposed and its corrosion resistance deteriorated dramatically. However, the effect of stressing on the stability of S-phase has not yet been investigated. Therefore, it is necessary to study the stability under using environments, like stress, temperature to understand the mechanism of its high performance, which forms the purpose of this research.

2 EXPERIMENTAL

The material investigated was hot rolled 316 stainless steel sheet with a thickness of 3mm, the chemical composition of which was listed in Table 1. The samples were cut to a conventional 'dog-bone' shape by electric discharge machining (Fig. 1). Carburizing treatment was carried out in a 60kW Klöchner DC plasma vacumm unit at 500°C for 10 hours in a 400Pa gas mixture of 1.5%CH_4 and 98.5% H_2 (coded as PC 10h hereafter).

Table 1. Composition of the 316 stainless steel sheet (wt%)

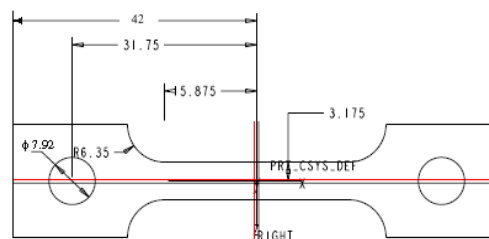| C	Cr	Ni	Mn	Mo	Si	Fe
0.03	17.35	10.34	1.62	1.86	0.69	Balance

Figure 1. Schematic drawing of specimen.

To study the thermo-mechanical stability of the S-phase, specimens were positioned within the grips and heated to test temperatures in a creep tester with different loads. The different testing parameters are listed in Table 2. The thermo-

mechanical stability tests were carried at temperatures between 400 and 500°C for 100-150h under a tensile stress up to 200MPa.

Table 2. Conditions for thermo-mechanical stability testsL

Samples Code	Temperature (°C)	Tensile Stress (MPa)	Enduring Time(h)
PC 10h*	0	0	0
PC400 0MPa	400	0	150
PC400 100MPa	400	100	150
PC400 200MPa	400	200	150
PC450 0MPa	450	0	100
PC450 100MPa	450	100	100
PC450 200MPa	450	200	100
PC500 0MPa	500	0	100
PC500 100MPa	500	100	100
PC500 200MPa	500	200	100

* As-carburised sample

Specimens were systematically characterized before and after the thermo-mechanical stability tests using Philips XL30 scanning electron microscope (SEM), Jeol 7000 field Emission Gun SEM with wavelength dispersive X-ray spectrometry(WDS), Philips X'Pert diffractometer and FEI Tecnai F20 Field emission transmission electron microscopy (TEM). The hardness was measured by a Mitutoyo MVK-H1 micro-hardness tester.

3 RESULTS

3.1 Evolution of Layer Morphology

Fig. 2 shows the cross-sectional SEM micrograph in a featureless homogenous S-phase layer formed during plasma carburizing at 500°C for 10h. No significant change in layer morphology was observed when the PC 10h sample was annealed at 400°C for 150h under tensile stresses ranging from 0 to 200MPa.

Comparing Fig. 2 with Fig. 3a & 4a reveals that the surface layer of the as-carburised PC 10h sample was increased following 100h annealing at 450 and 500°C. In general, it is apparent that the surface layer was expanded with the increment of temperature and stress.
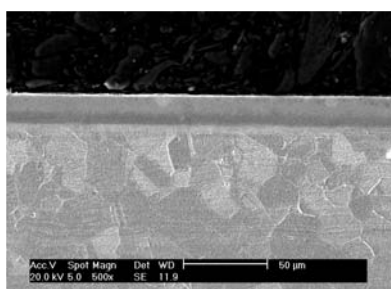

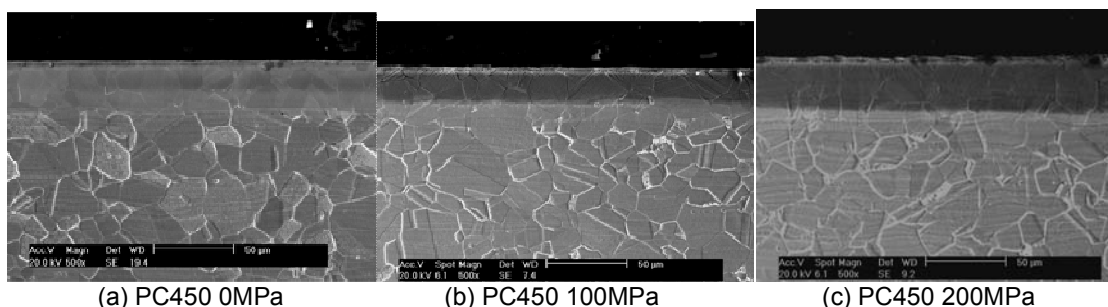**Figure 2.** SEM micrograph of carburised sample.

| (a) PC450 0MPa | (b) PC450 100MPa | (c) PC450 200MPa |

Figure 3. SEM cross-sectional morphologies of 450 °C annealed samples under (a) 0MPA, (b) 100MPa and (c) 200MPa.

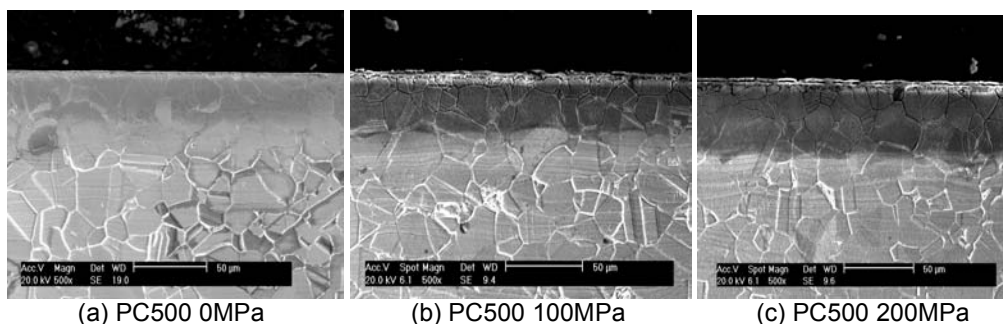| (a) PC500 0MPa | (b) PC500 100MPa | (c) PC500 200MPa |

Figure 4. SEM cross-sectional morphologies of 500 °C annealed samples under (a) 0MPA, (b) 100MPa and (c) 200MPa.

When annealed under tensile stress a very thin superficial layer was clearly seen for both 450°C/100h and 500°C/100h annealed samples, the thickness of which was increased with increasing the tensile stress from 100 to 200MPa. In addition, the contrast between the main surface layer and the substrate became larger when annealed under tensile stress. The grain boundaries and slipping bands can be easily seen in the stressed 500°C/100h annealed samples

3.2 Phases and Lattice Parameters

XRD analysis was conducted on all the samples and Fig. 5a shows the XRD charts of 316 substrate (UT316), as-carburised sample (PC 10h) and 500°C/100h stressed (PC500 0MPa, PC500 100MPa, PC500 200MPa) samples.

As observed by previous researchers,[9] the carburized samples illustrated left-shift of peak positions comparing with the typical 316 stainless steel indicating the formation of carbon supersaturated expanded austenite (i.e. S-phase layers). Minor peaks of iron oxides Fe_2O_3 and Fe_3O_4 were identified from the XRD charts for the 500°C/100h annealed samples especially when they were stressed. This is in line with the existence of the very thin superficial layer shown in Fig. 4. These oxides were formed due to oxidation of the sample surfaces during the 500°C/100h, and the applied tensile stresses promoted the formation of such oxide layers. No precipitation peaks were detected by the X-ray diffratograms.

The lattice parameter of the expanded austenite in the S-phase layers was obtained by the plot of $a_{(hkl)}$ against $\cos \theta_{(hkl)} * \cot \theta_{(hkl)}$, where $a_{(hkl)}$ is the lattice parameter value estimated from the peak indexed by (hkl) and $\theta_{(hkl)}$ is the Bragg angle. Fig. 5b shows a Nelson-Riey plot obtained from all the X-ray diffraction. All the experimental data for the annealed samples fall between that for the untreated 316

and that for carburized samples (fitted by lines). There exists a tendency that with increasing temperature and stress, the lattice parameter $a_{(hkl)}$ approaches the untreated state.
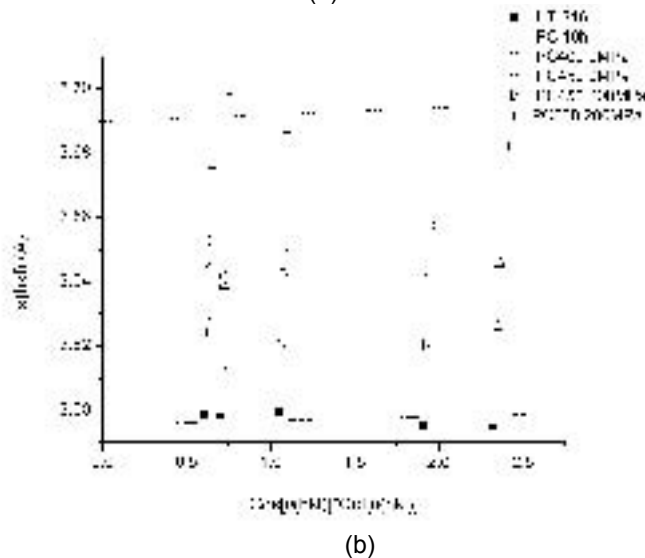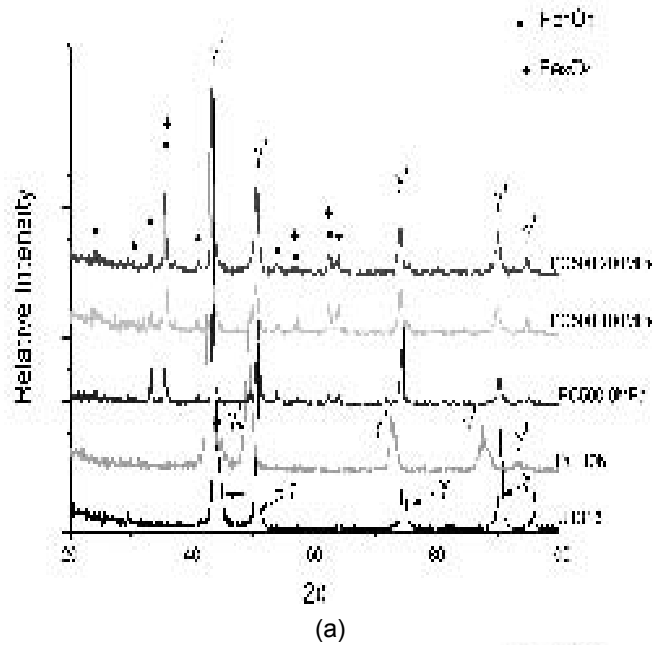

(a)

(b)

Figure 5. XRD charts (a) and Nelson-Riley plot (b) for 316 substrate (UT316), as-carburised (PC 10h) and thermomechanically tested samples.

3.3 Carbon and Hardness Distribution

The carbon concentration was quantified by WDS and the results revealed that the carbon atoms dissipated during the thermo-mechanical stability tests. Without stressing, the surface carbon concentration reduced from 3.8 wt.% for the as-carburised surface to 1.0wt.% and 0.75wt.% respectively for the 400°C/150h and 500°C/100h treated samples. In addition, it seems that the tensile stress has a positive effect on the retardation of carbon reduction in the surface. For example, the

surface carbon content was 0.7 and 1.5 wt% for PC 500 0MPa and PC 500 200MPa respectively.

The effect of the thermo-mechanical tests on the hardness distribution is depicted in Fig. 6. In general, the hardness of the plasma carburized sample reduced after the thermo-mechanical tests. This is mainly because without the constant supply of carbon, the supersaturated carbon in S-phase underwent diffusion both outward and inward, thus reducing its hardness. However, two interesting features were notice from Fig. 6. First, whist the low- and-medium temperature annealed samples, whether stressed or not, showed a gradual reduction of the hardness with the depth, the high-temperature treated samples displayed a sigmoid distribution. This implies that decarburising may have occurred at temperatures above $450^{\circ}C$.
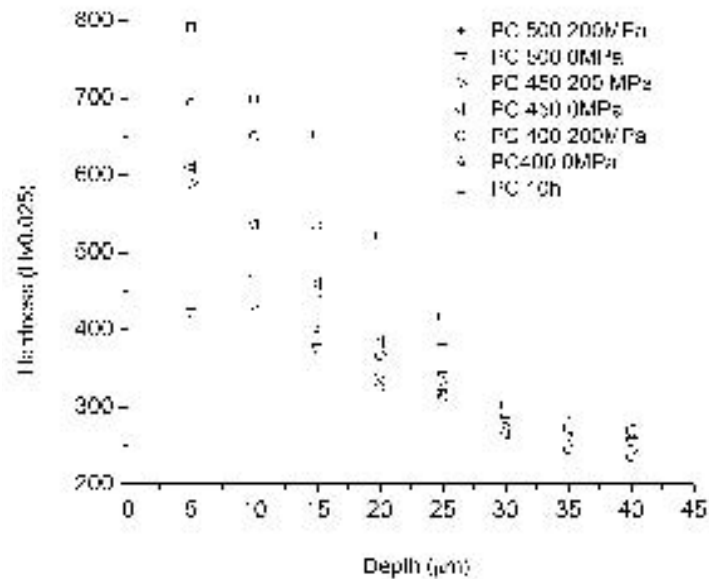

Figure 6. Hardness vs. depth profiles.

Second, the application of a tensile stress during annealing of S-phase layer can retard the deduction of its hardness in particular for the 400 and $500^{\circ}C$ annealed samples. For example, the hardness at the depth of 20 microns was about 320HV0.025 for PC 500 0MPa (without applied stress) while that of PC 500 200MPa (with 200MPa applied stress) was about 520HV0.025, which is the same as that for the as-carburised sample (PC 10h). It could reasonably be deduced that very fine precipitates may have been formed at the grain boundaries or twin boundaries, thus producing precipitation hardening. This may also account for the observed slightly reduced corrosion resistance and the deeply etched grain boundaries as observed in Fig. 3.

This precipitation was most probably facilitated by the applied tensile stresses since the hardness of PC 500 0MPa reduced significantly after $500^{\circ}C$ /100h annealing without stressing and no corrosion loss or deeply etched grain boundaries were observed for this sample (Fig. 4a). It is known that S-phase is highly compressively stressed,[10] which could potentially delay the precipitation; applying a tensile stress can partially cancel out the compressive stress and thus promote the

formation of precipitates. However, this may be at the early stage of precipitation and therefore XRD failed to show any peaks of potential precipitates. TEM investigation is undertaking to further verify the above assumption.

4 SUMMARY AND CONCLUSION

The stability of S-phase is a critical issue for industrial applications owing to its metastable nature. In this study, the stability of S-phase under both thermal and mechanical conditions has been investigated. The experimental results demonstrate that when stressed at 400°C for 150h the microstructure of the carbon S-phase was not affected by the stress levels up to 200MPa; however, when stressed at 450 and 500°C for 100MPa or above, the corrosion resistance of the carbon S-phase was slightly reduced as evidenced by the dark colour and deep etched grain boundaries. The application of a tensile stress during annealing of S-phase layer can retard the deduction of its hardness. This is believed to be related to the early stage precipitation of carbides in the S-phase, which could be facilitated by the applied tensile stress during thermal annealing.

REFERENCES

1   J.P. Lebrun, European Patent EP 1000181, 02-01-2002.
2   Y. Cao, F.Ernest and G.M. Michal, Acta Materialia, v.51, p.4171-4181, 2003.
3   Z.L. Zhang and T. Bell, Surface Engineering, v.1, 131-136, 1985.
4   K. Ichii et al., Technology Report of Kansai University, v.27, p.135-144, 1986.
5   T. Christiansen, M.A.J Somers, Scripta Materialia, v.50,p. 35-37, 2004.
6   G.M. Michal , F. Ernst, H. Kahn, Y. Cao et al., Acta Materialia, v. 51 p.1597-1606, 2006.
7   H. Dong, International Materials Review, v.55, p.65-98,2010.
8   X.Y. Li, H. Dong. Materials Science and Technology, v.19, p.1427-1434, 2003.
9   S. Thaiwatthana, X.Y. Li, H. Dong, T. Bell, Surface Engineering, v.18, p.433-437, 2002.
10   T. Christiansen, K.V. Dahl, M.A.J Somers, Materials Science and Technology, v. 24, p.159-167, 2008.